

# A numerical exact solution of the Bose-Hubbard model

N. Elstner and H. Monien

*Physikalisches Institut, Universität Bonn, Nußallee 12, D-53115 Bonn, Germany*

(November 26, 2024)

In this paper we report results from a systematic strong-coupling expansion of the Bose-Hubbard model in one and two spatial dimensions. We obtain numerically exact results for the structure factor and the spectrum of single particle and single hole excitations in the Mott insulator. This enables the determination of the zero-temperature phase diagram and the location of the critical endpoints of the Mott lobes. In one dimension we confirm the occurrence of reentrance behavior from the compressible to the insulating phase in a region close to the critical point.

PACS numbers: 05.30.Jp, 05.70.Jk, 67.40.Db

## I. INTRODUCTION

Quantum phase transitions in strongly correlated systems have attracted a lot of interest in recent years. Here we focus on systems of interacting bosons. Physical realisations include Josephson junction arrays, granular and short-correlation-length superconductors, flux-lattices in type-II superconductors and possibly in the future ultra-cold atoms in a periodic potential.

The minimal model containing the key feature of competition between kinetic and potential energy is the Bose-Hubbard hamiltonian. It is given by

$$H = -t \sum_{\langle i,j \rangle} (b_i^\dagger b_j + b_j^\dagger b_i) + U \frac{1}{2} \sum_i \hat{n}_i(\hat{n}_i - 1) - \mu \sum_i \hat{n}_i \quad (1)$$

where the  $b_i^\dagger$  and  $b_i$  are bosonic creation and annihilation operators,  $\hat{n}_i = b_i^\dagger b_i$  is the number of particles on site  $i$ ,  $t$  the hopping matrix element,  $U > 0$  the on-site repulsion and  $\mu$  the chemical potential.

This model has been studied previously by Quantum Monte Carlo simulations<sup>1,2,3,4,5,6,7</sup> in one and two spatial dimensions. Recently the one-dimensional case was also investigated using the density-matrix renormalisation group (DMRG). This study found indications for reentrance from the superfluid to the Mott-insulator for certain parameter values.

The zero-temperature phase diagram can be understood by starting from the strong-coupling or “atomic” limit where the kinetic energy term vanishes ( $t = 0$ ). In this limit the ground state is an insulator with a fixed number  $n_0$  of particles per site and the wavefunction is given by

$$|n_0\rangle_{\text{Mott}}^{(0)} = \prod_{i=1}^N \frac{1}{\sqrt{n_0!}} (b_i^\dagger)^{n_0} |0\rangle \quad (2)$$

with energy

$$E_{\text{Mott}}^{(0)}/N = U \frac{1}{2} n_0(n_0 - 1) - \mu n_0 \quad (3)$$

Single charge excitations in the atomic limit are created by adding or removing a particle onto or from a particular site  $i$ :

$$|n_0; i\rangle_{\text{part}}^{(0)} = \frac{1}{\sqrt{(n_0 + 1)}} b_i^\dagger |n_0\rangle_{\text{Mott}}^{(0)} \quad (4)$$

$$|n_0; i\rangle_{\text{hole}}^{(0)} = \frac{1}{\sqrt{n_0}} b_i |n_0\rangle_{\text{Mott}}^{(0)} \quad (5)$$

The energy of these states relative to the ground state is given by

$$E_{\text{particle}}^{(0)} = U n_0 - \mu \quad (6)$$

$$E_{\text{hole}}^{(0)} = -U(n_0 - 1) + \mu \quad (7)$$

for particle and hole excitations respectively. For certain critical values of the chemical potential  $\mu_c^{(0)} = U n_0$  this energy vanishes and the system becomes compressible. If the hopping matrix element  $t$  is finite the range of the chemical potential for which the system is incompressible decreases. At some critical value  $t_c$  of the hopping matrix element the Mott insulator will completely disappear. The resulting phase diagram shows Mott insulating regions, usually referred to as Mott lobes, surrounded by a compressible phase.

This phase is characterized by the following real space correlation function:

$$S_j = \langle b_j^\dagger b_0 + b_j b_0^\dagger \rangle \quad (8)$$

In spatial dimension  $D > 1$  the correlations are long ranged and the system is a superfluid, while in one dimension it is a Luttinger Liquid with  $S_j$  decaying algebraically for large distances. In this article we will investigate the Fourier transform

$$S(\mathbf{q}) = \sum_j e^{i\mathbf{q} \cdot \mathbf{r}_j} S_j \quad (9)$$

and it's second moment

$$m_2(\mathbf{q}) = -\frac{\partial^2}{\partial \mathbf{q}^2} S(\mathbf{q}) \quad (10)$$

Assuming a lorentzian shape of  $S(\mathbf{q})$  near the ordering wave vector  $\mathbf{q} = 0$  the correlation length,  $\xi$ , is given by

$$\xi^2 = \frac{m_2(\mathbf{q} = 0)}{S(\mathbf{q} = 0)} \quad (11)$$

We used strong coupling expansions in  $t/U$  to calculate the ground state energy,  $E_0$ , the spectrum of single charge excitations  $E_{particle/hole}(\mathbf{q})$ , the correlation function  $S(\mathbf{q})$  and the correlation length  $\xi$ . The resulting series were analysed using Padé extrapolation techniques.

In the next section we give a technical outline of how to calculate the ground state energy,  $E_0$ , the spectrum of single charge excitations  $E_{particle/hole}(\mathbf{q})$ , the correlation function  $S(\mathbf{q})$  and the correlation length  $\xi$  by strong coupling expansions in  $t/U$ . We use methods that had been developed over the last decade but so far were mainly applied to spin systems.

Section III focusses on the ground state and the excited states. We present the dispersion of the single particle excitations and the dependence of the particle-hole gap on the hopping amplitude  $t$ . It is found that the series converges rather fast provided  $t$  is smaller than the critical value  $t_c$ . In this regime, the Mott insulator, we obtain the numerical exact single charge excitation spectrum.

In the following section the phase diagram in two dimensions is discussed. Again due to the rapid convergence of the series it is possible to determine numerically exact the boundary of the Mott lobes. Only in a small region close to the critical point  $t_c$  does the convergence break down and series extrapolation techniques have to be applied. These also work extremely well and it is thus possible to determine the critical point with high accuracy. We also determine the critical exponents and find that they agree with the field theoretic predictions that this  $D$ -dimensional quantum system is in the universality class of the  $D + 1$ -dimensional classical xy-model.

Section V deals with the special case of a one-dimensional system. As already mentioned the compressible phase exhibits only quasi longrange order. Also the phase transitions at the top of the Mott lobes changes qualitatively and becomes of the Bereshinski-Kosterlitz-Thouless (BKT) type. Our analysis of the phase diagram finds a reentrance behaviour, i.e. for a certain range of values of the chemical potential the system has not just one transition from the Mott state to the compressible phase but upon further increase of the hopping strength  $t$  becomes insulating again until a second transition to the liquid occurs. This scenario agrees with recent DMRG calculations. We give a simple intuitive explanation for this surprising observation.

Conclusion

## II. SERIES EXPANSION TECHNIQUE FOR EXCITED STATES

Strong coupling perturbation theory can be formulated as a linked cluster expansion, see e.g.<sup>8</sup>. For the ground state energy this is basically nondegenerate Rayleigh-Schrödinger perturbation theory performed for every cluster contributing up to a certain order in the expansion. In order to obtain correlation function one has to formally add source terms,

$$H_{\text{source}} = \sum_{i,j} J_{i,j} \left( b_i^\dagger b_j + b_i b_j^\dagger \right) \quad , \quad (12)$$

to the hamiltonian and expand the energy to linear order in the  $J_{i,j}$ . Differentiating with respect to the source fields will give the strong coupling expansion for the correlation functions. This procedure is necessary, because it is not possible to evaluate the wave function directly by a linked cluster expansion. This is due to the fact that the linked cluster theorem applies only to physical observables that are additive when the system separates into disconnected part.

A systematic strong coupling expansion of the energy of the charge excitations complicated due to the high degeneracy. The problem how to write down a linked cluster expansion for degenerate states was solved only recently by Gelfand<sup>9</sup>. The idea is to construct perturbatively an effective Hamiltonian  $H_{i,j}^{\text{eff}}$  in the subspace of the degenerate states  $|n_0; i\rangle_{\text{part/hole}}^{(0)}$  by a similarity transformation

$$H_{i,j}^{\text{eff}}(t) = S_{i,\nu}(t) H_{\nu,\lambda} S_{\lambda,j}(t) \quad (13)$$

with  $S_{i,\nu}(t) = S_{\nu,i}^{-1}(t)$

where Greek indices run over states in the full Hilbert space while Latin indices are restricted to the degenerate manifold of single particle and single hole states (4) and (5) respectively. Then the linked cluster theorem applies to  $H_{i,j}^{\text{eff}}(t) - E_{\text{Mott}}(t)$ . In the case of a homogeneous system  $H_{i,j}^{\text{eff}}$  depends only on the difference of indices  $i - j$  and is easily diagonalised by a Fourier transform. This way one can determine the full dispersion  $E(\mathbf{q}; t, \mu)$  of the charge excitations. In many ways the linked cluster expansion is similar to an exact diagonalization study of small systems - however in the linked cluster expansion it is possible to remove all finite size effects in each order and one obtains the full dispersion in the thermodynamic limit.

We close this section with some technical remarks. Expansions were performed up to 13<sup>th</sup> order for the triangular lattice with 12,253 clusters contributing. The Hilbert-space of the largest cluster had 37,442,160 states in the single particle sector with filling  $n_0 = 1$ . Up to 13<sup>th</sup> order in perturbation theory just a fraction of these states (788,238) actually contribute to the expansion. It was only after we restricted the calculation to this

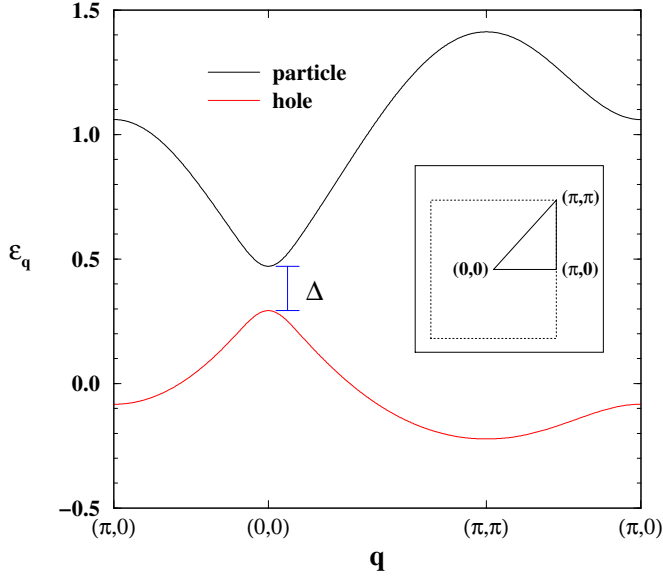


FIG. 1. Dispersion of the single-particle and single-hole excitations of the square lattice Bose-Hubbard model at  $t/U = 0.055$

subset of relevant states that it was possible to perform this work. Any significant improvement is unlikely because the Hilbert-space and the number of clusters both increase exponentially with the order of the expansion.

### III. GROUND STATE AND SINGLE CHARGE EXCITATIONS

We will first discuss the two dimensional case. We investigated both the square and triangular lattice and calculated the series for occupation numbers  $n_0 = 1$  and  $n_0 = 2$  up to 13<sup>th</sup> and 10<sup>th</sup> order respectively.

The spectrum  $E(\mathbf{q}; t, \mu)$  takes on the form

$$E_{\text{part}}(\mathbf{q}; t, \mu) = \epsilon_{\text{part}}(\mathbf{q}; t) - \mu \quad (14)$$

$$E_{\text{hole}}(\mathbf{q}; t, \mu) = -\epsilon_{\text{hole}}(\mathbf{q}; t) + \mu \quad (15)$$

in complete analogy to eqns. (6) and (7). For positive values of the hopping matrix element  $t$  the smallest (largest) eigenvalue in the particle (hole) sector is always located at wavevector  $\mathbf{q} = 0$ . The upper and lower phase boundaries of the Mott phase are thus given by  $\mu_{\text{upper}}(t) = \epsilon_{\text{part}}(\mathbf{q} = 0; t)$  and  $\mu_{\text{lower}}(t) = \epsilon_{\text{hole}}(\mathbf{q} = 0; t)$ , respectively.

As a consequence the single charge gap  $\Delta(t) = \epsilon_{\text{part}}(\mathbf{q} = 0; t) - \epsilon_{\text{hole}}(\mathbf{q} = 0; t)$ , determines also the width  $\mu_{\text{upper}}(t) - \mu_{\text{lower}}(t)$  of the insulating region. With increasing hopping  $t$  the distance between the upper and lower boundary decreases until finally at some critical value,  $t_c$ , the energy to remove a particle and the energy to add a particle become degenerate and the Mott insulator vanishes altogether.

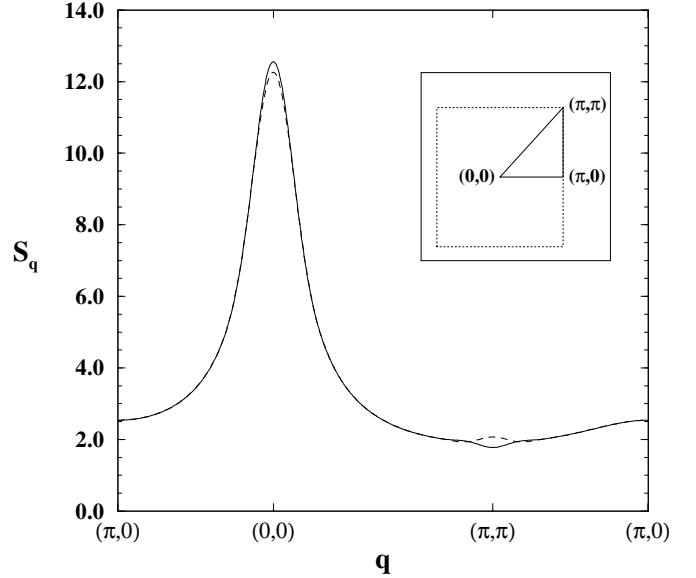


FIG. 2. Correlation function  $S(k)$  of the square lattice Bose-Hubbard model at  $t/U = 0.055$

The dispersion of the particle and hole excitations for  $n_0 = 1$  on the square lattice and triangular lattice is shown in Figs. 1 and 3. The different shape of the two curves reflects the particle-hole asymmetry of the model hamiltonian (1). The series were found to converge very fast. Both Figures were obtained by summation of the 13<sup>th</sup> order series. They turned out to be almost indistinguishable from the result of the 10-term series even for  $t/U = 0.055$  (square lattice) and  $t/U = 0.035$  (triangular lattice) which is not far from the critical endpoints  $t_c$  of the first Mott lobe for these two lattices. The particle and hole excitations both have a pronounced extremum at wavevector  $\mathbf{q} = 0$  and are separated by a gap  $\Delta$ . For values of the chemical potential  $\mu$  in this range all single charge excitations are gapped and the system is insulating. Coefficients of the series expansion of  $\Delta$  are given in Tab.(1).

Figs.2 and 4 show the correlation function  $S(\mathbf{q})$  for the same sets of parameters as for the dispersion. Although the system is still in the Mott phase there is already a pronounced peak at wavevector  $\mathbf{q} = 0$ .

### IV. 2D PHASE DIAGRAM

The phase diagram can be obtained from the series for the single charge excitations. Outside the critical region the values of the chemical potential for which the system becomes compressible can be directly calculated from the series. Only near the critical point is it necessary to use extrapolation methods. We applied a Pade analysis and obtained the phase diagrams shown in Figs.5 and 5 for the square and triangular lattices. With the excep-

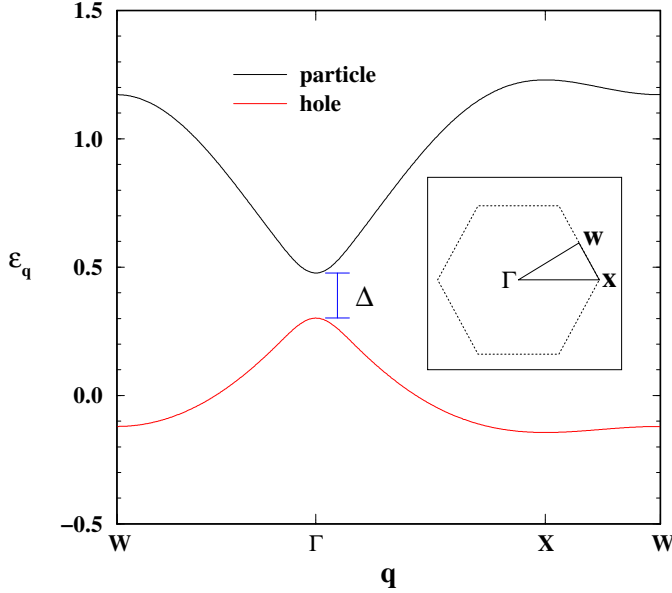


FIG. 3. Dispersion of the single-particle and single-hole excitations of the triangular lattice Bose-Hubbard model at  $t/U = 0.035$

tion of the lowest approximand all others turn out to be almost indistinguishable again indicating rapid convergence.

The bare series shows a remarkable fast convergence for not too large values of the expansion parameter. In each order  $k$  of the expansion  $\Delta$  vanishes at some effective critical value  $t_c(k)$  with a corresponding effective  $\mu_c(k)$ . Plotting  $t_c(k)$  and  $\mu_c(k)$  vs.  $1/k$  one finds again a rapid convergence as shown in Figs.(7) and (9). Extrapolation to  $n \rightarrow \infty$  allows to determine accurately the critical point:

$$t_c = 0.05974 \pm 0.00004 \quad (\text{square lattice}) \quad (16)$$

$$t_c = 0.037785 \pm 0.000005 \quad (\text{triangular lattice}) \quad (17)$$

The accuracy for the triangular lattice is almost an order of magnitude better than for the square lattice. This is because the series for the triangular lattice has a monotonic convergence while the square lattice shows an oscillatory behaviour between even and odd terms as can be seen when comparing Figs.(7) and (9). The convergence of the data is significantly accelerated when considering the difference between neighbouring data points. Fitting each pair of points  $t_c(k)$  and  $t_c(k-1)$  to a linear function  $t_c^{(1)}(k) + a(k)/k$  removes the leading  $1/k$  dependence and gives an even faster converging new sequence of points  $t_c^{(1)}(k)$ . For the triangular lattice the result is shown in Fig.(10). Without further extrapolation this confirms the above value of the critical point.

Having located  $t_c$  we now turn to a more detailed investigation of the critical behaviour. Scaling theory predicts this phase transition to be in the universality class

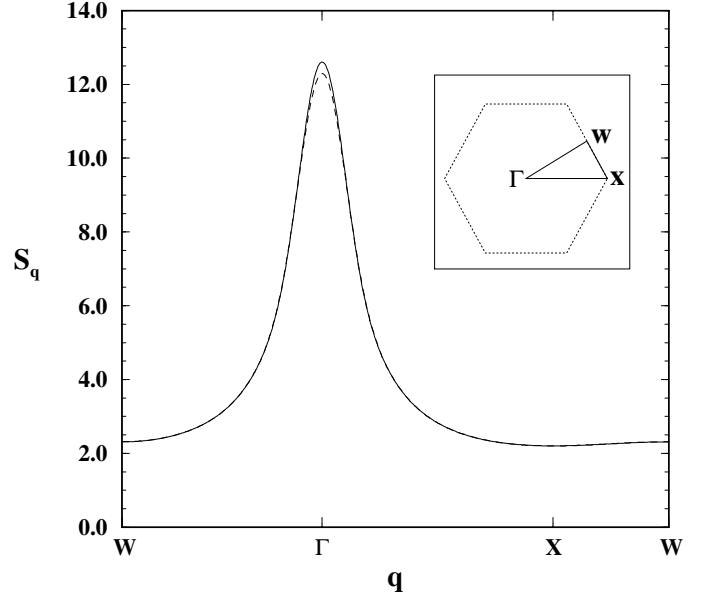


FIG. 4. Correlation function  $S(k)$  of the triangular lattice Bose-Hubbard model at  $t/U = 0.035$

of the three-dimensional xy-model<sup>10</sup>. The Mott lobe is thus expected to close following a power law

$$\Delta(t) \propto (t_c - t)^{z\nu}, \quad (t_c - t) \ll 1. \quad (18)$$

where  $z$  the dynamical exponent is given by  $z = 1$ . From the scaling form of the dynamic susceptibility<sup>10</sup> the power law divergence of the static structure factor can be derived

$$S(q=0, t) \propto (t_c - t)^{\gamma_s}, \quad (t_c - t) \ll 1 \quad (19)$$

$$\text{with } \gamma_s = (1 - \eta)\nu \quad (20)$$

We used a Dlog-Pade analysis to check these scaling predictions. For the square lattice this gives for the critical point  $t_c \approx 0.0598$  and the critical exponents  $\nu \approx 0.69$  and  $\gamma_s = 0.653$ . The different Padé approximants differ quite a bit and the  $t_c$  value clearly does not agree with the result of the  $1/n$  extrapolation. The values for the critical exponent  $\nu$  have to be compared with the known value for the 3D xy-model<sup>13</sup>,  $\nu = 0.6693 \pm 0.0010$  and  $\gamma_s = 0.64 \pm 0.0022$ , obtained by Borel summation of field theoretical results. Also the difference between the two results is quite small of the order of a few per cent this is still closer to the 3D Heisenberg model with  $\nu = 0.7054 \pm 0.0010<sup>13</sup> than to the xy-result. The convergence for the square lattice is not that good as mentioned before. When going to triangular lattice the accuracy of the analysis improves significantly. The Dlog-Pade approximants find the critical point at  $t_c \approx 0.03778$  with exponent  $\nu = 0.681 - 0.683$  and  $\gamma_s = 0.651 - 0.652$ . The values for different approximants are presented in Tab. B. The  $t_c$  value is in excellent agreement with the  $1/n$$

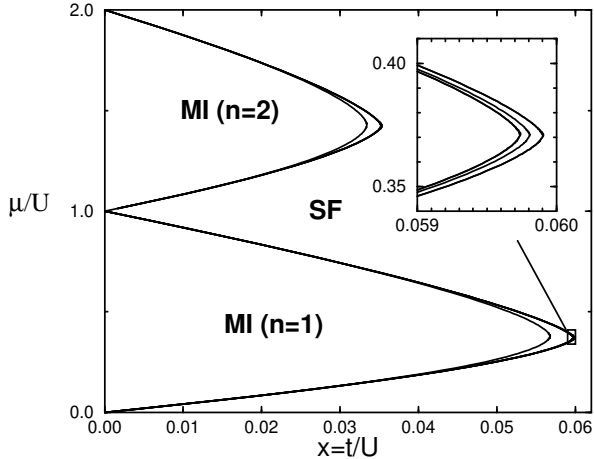


FIG. 5. Square lattice: Phase Diagram obtained by Pade analysis.

extrapolation. The critical exponent still remains higher than the field theoretic value. Looking carefully at the values for  $t_c$  and  $\nu$  as given by different approximants there is a tendency for both quantities to decrease slowly with increasing length of the series. In addition to the standard Dlog-Pade analysis we also performed a biased analysis with the critical point fixed at  $t_c = 0.03778$ . This gave  $\nu = 0.6805 - 0.6810$ .

The critical exponent depends linearly on the critical point. Fixing  $\nu$  at its field theoretic value this would require  $t_c = 0.03775 - 0.03776$  which can clearly be ruled out by the  $1/n$  extrapolation.

The discrepancy is probably due to subleading corrections to the asymptotic divergent term. The Dlog-Pade analysis ignores these contributions and assumes a pure power law divergence at the critical point. An improved analysis to resolve this subtle question however would require much longer series which won't be possible, because the numerical problem grows exponentially with the order of the series.

## V. 1D PHASE DIAGRAM

We now turn to the one-dimensional case. Scaling theory<sup>10</sup> predicts the critical behavior of the system to be that of a Kosterlitz-Thouless transition for which the Mott lobes closes according to

$$\Delta(t) \propto A \exp\left(-\frac{W}{\sqrt{t_{KT} - t}}\right), \quad (t_{KT} - t) \ll 1. \quad (21)$$

This highly nonanalytic behavior renders a direct series extrapolation complicated and the results of such a simpliminded approach are not conclusive. In order to determine the phase diagram we thus performed a Pade

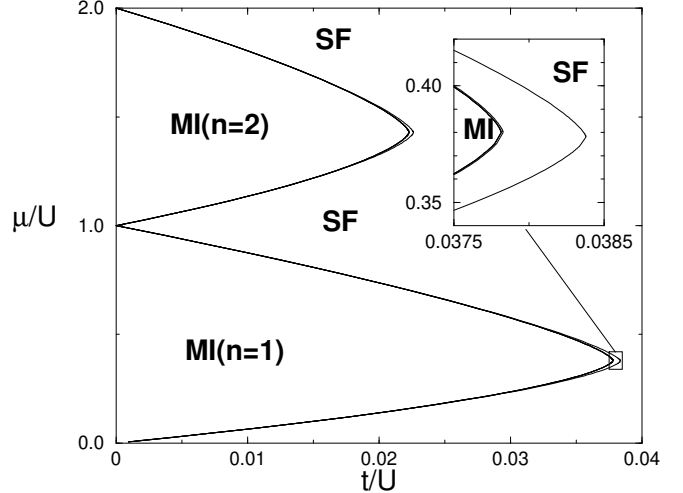


FIG. 6. Triangular lattice: Phase Diagram obtained by Pade analysis.

analysis for  $\ln^2 \Delta(t) \propto (t_{KT} - t)^{-1}$ . This quantity has a simple pole at the critical point which can be captured by a rational function.

The phase diagram obtained this way is shown in Fig.11 where we compare results from the series analysis with numerical data of QMC simulations by Batrouni and Scalettar<sup>2</sup> and a recent DMRG study<sup>11,12</sup>. The agreement between the series and the DMRG data is excellent. Quite remarkable is the reentrance behavior found for  $t/U > 0.2$ . The series analysis thus confirms this phenomenon first observed in the DMRG calculation. This type of behavior is a new feature not seen before in investigations of Bose systems.

A simple intuitive way of understanding this phenomenon is the fact that Mott lobe is particle-hole asymmetric for the lattice problem. Starting from strong coupling ( $U \gg t$ ) it is clear that the effect of the kinetic energy is to delocalize the particles. The delocalization decreases the average number of particles per site if the chemical potential is held fixed. On the other hand in the weak coupling limit ( $U \ll t$ ) the bosons condense at the lower band edge so that for increasing bandwidth ( $t$ ) and fixed chemical potential the average number of particles per site is decreasing. The nonmonotonic behavior of the density can be understood simply as a result of two limiting cases. Thus starting from the Mott phase the number of particles per site first decreases and then increases leading to a second Mott transition for a well defined range of the chemical potential. **plot of  $n = \text{const.}$  lines in mean field ?**

The uncertainties in the precise location of the Kosterlitz-Thouless transition are still comparatively large. We use a Pade analysis of  $\ln^2 \Delta(t) \propto (t_{KT} - t)^{-1}$ . This methods turned out to give excellent results. We estimate the point for Kosterlitz-Thouless transition to be

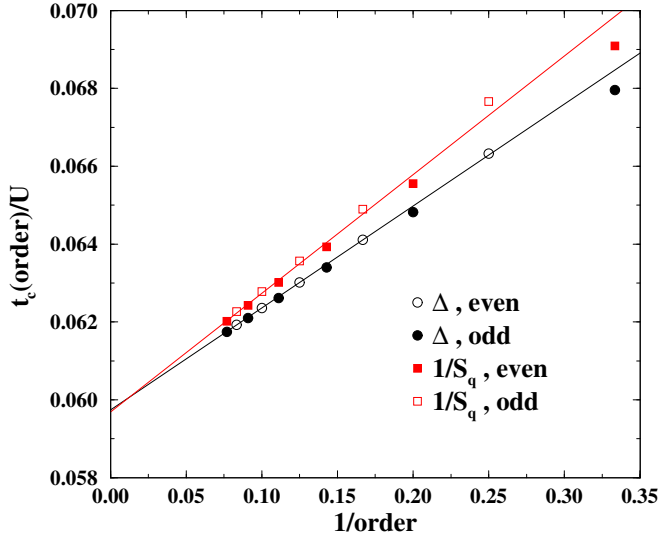


FIG. 7. Square lattice:  $1/k$  extrapolation of the critical point  $t_c$ . The circles and squares are estimates from series for the gap and correlation function respectively. Note the excellent agreement between the  $t_c$  estimates of these two independent quantities.

located at  $t_{KT}/U = 0.26 \pm 0.01$  and  $\mu_{KT}/U = 0.16 \pm 0.01$ .

## VI. CONCLUSION

In conclusion, series expansion techniques were applied to investigate the zero temperature properties of the Bose-Hubbard model. We determine the complete spectrum of single-particle and single-hole excitations in the Mott phase. The phase diagram in one and two dimensions is obtained and the critical end points of the Mott insulator regions are determined. In two dimensions this is so far the only investigation of the complete phase diagram of this problem. In one dimensions the series shows almost perfect agreement with a recent DMRG study and provides a conclusive confirmation for reentrance behavior from the compressible to the insulating phase near the Kosterlitz-Thouless point.

We acknowledge useful and interesting discussions on this problem with M. P. Gelfand, T. Giamarchi, T. Kühner, A. J. Millis, R. Noack, A. v. Otterlo, R. R. P. Singh, U. Schollwöck, G. Schön, H. Schulz, and S. R. White

## APPENDIX A: EXPLICIT SERIES EXPANSION FOR SMALL CLUSTERS

Perturbation theory for physical observables can be formulated as a coupled cluster expansion, see e.g.<sup>8</sup>. This

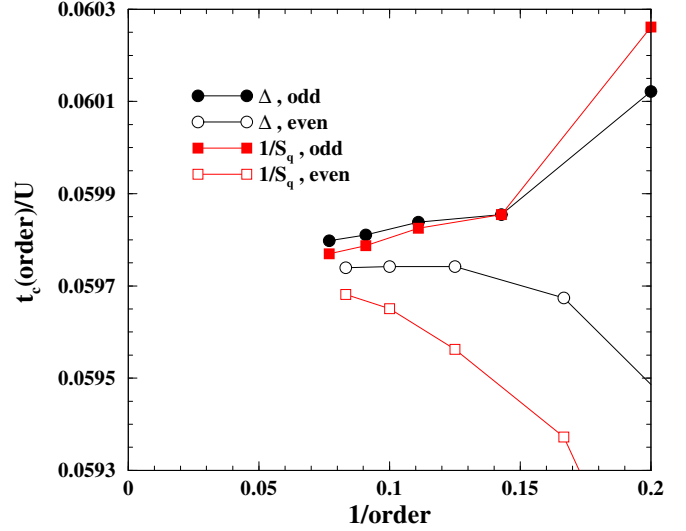


FIG. 8. Square lattice:  $1/n$  extrapolation of the critical point sequence  $t_c^{(1)}$ . Note the scale of the vertical axis!

allows to write the ground state energy for the Bose-Hubbard model on a particular lattice  $\mathcal{L}$  in the following way

$$E_{\text{Mott}}(\mathcal{L})/N = E_{\text{Mott}}^{(0)}/N + \sum_g L(g) \times W_E(g) \quad . \quad (\text{A1})$$

Here  $g$  are the connected clusters or graphs that can be embedded into the lattice  $\mathcal{L}$ , the so called lattice constant  $L(g)$  is the number of embeddings *per site* of  $g$  in  $\mathcal{L}$  and  $W_E(g)$ , the cluster weight, is the contribution of  $g$  to the expansion of the energy  $E$ . Each cluster represents itself a small lattice and the weights can be expressed by the recursion relation

$$W_E(g) = E_{\text{Mott}}(g) - \sum_{g' \subset g} W_E(g') \quad , \quad (\text{A2})$$

where  $E_{\text{Mott}}(g)$  is the ground state energy of the particular cluster  $g$  under consideration and the  $g'$  are all its subclusters. An important property of the weights is that

$$W_E(g) = \mathcal{O}(x^n) \quad , \quad (\text{A3})$$

for a cluster with  $n$  bonds ( $x = t/U$ ). The procedure to calculate the series for the ground state energy up to a certain order  $\mathcal{O}(x^n)$  is now straightforward: first one has to find all cluster with up to  $n$  bonds and determine their lattice constants  $L(g)$ , in the next step for each cluster its ground state energy  $E_{\text{Mott}}(g)$  has to be determined perturbatively from which the weights follow by eqn.(A2). Summing up all the contributions, eqn.(A1) gives the desired result.

As an example we briefly discuss the expansion for the Bose-Hubbard chain. The clusters that contribute are

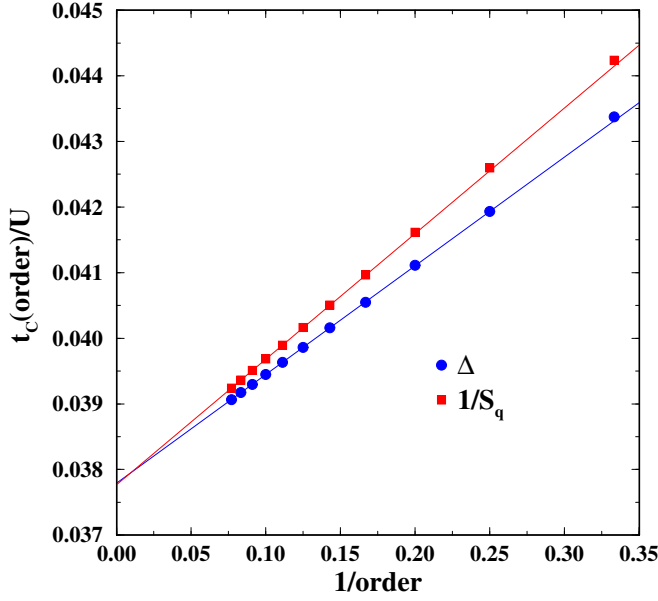


FIG. 9. Triangular lattice:  $1/k$  extrapolation of the critical point  $t_c$ . The circles and squares are estimates from series for the gap and correlation function respectively. Note the excellent agreement between the  $t_c$  estimates of these two independant quantities.

particular simple: finite open chains with  $n$  bonds and  $n + 1$  sites all having lattice constant  $L(g) = 1$ . The first three cluster that contribute have the following ground state energies:

$g$	$E(g)$
$\times \text{---} \times$	$-4x^2 + 16x^4 - 128x^6$
$\times \text{---} \times \text{---} \times$	$-8x^2 + 20x^4 + \frac{40}{3}x^6$
$\times \text{---} \times \text{---} \times \text{---} \times$	$-12x^2 + 24x^4 + \frac{392}{9}x^6$

Nest step is the subcluster subtraction: the one bond cluster can be embedded two (three) times into two (three) bond cluster and the two bond cluster also two times into the three bond cluster. This gives for the weights:

$g$	$W_E(g)$
$\bullet \text{---} \bullet$	$-4x^2 + 16x^4 - 128x^6$
$\bullet \text{---} \bullet \text{---} \bullet$	$-12x^4 + \frac{808}{3}x^6$
$\bullet \text{---} \bullet \text{---} \bullet \text{---} \bullet$	$-\frac{1000}{9}x^6$

Summing up all these different term gives the series for

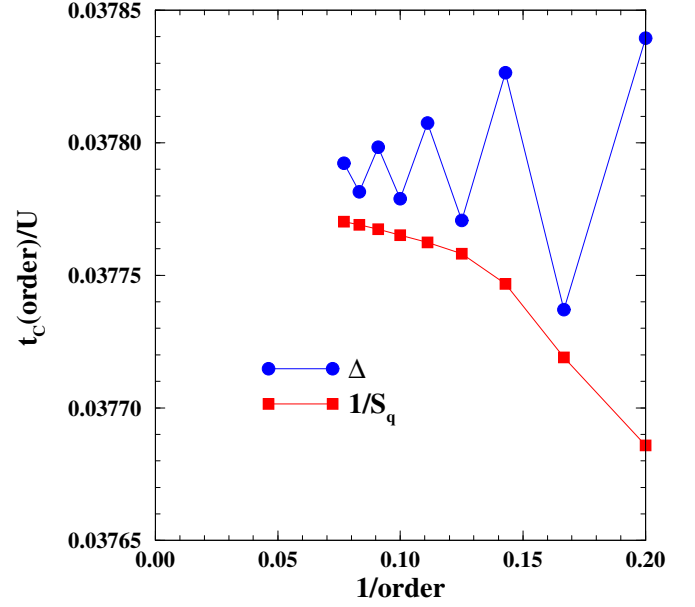


FIG. 10. Triangular lattice:  $1/n$  extrapolation of the critical point sequence  $t_c^{(1)}$ . Note the scale of the vertical axis!

the ground state energy:

$$E_{\text{Mott}}(\mathcal{L} = 1D)/N = -4x^2 + 4x^4 + \frac{272}{9}x^6$$

We now turn to the construction of the effective hamiltonian for the excited states. As an example we will discuss the single particle states, eqn.(4). The effective hamiltonians obtained by degenerate perturbation theory for the clusters with up to three bonds are given below. Note that the energies are given with respect to the ground state energy, because the coupled cluster theorem applies only to the difference  $H_{\text{eff}} - E_0$ .

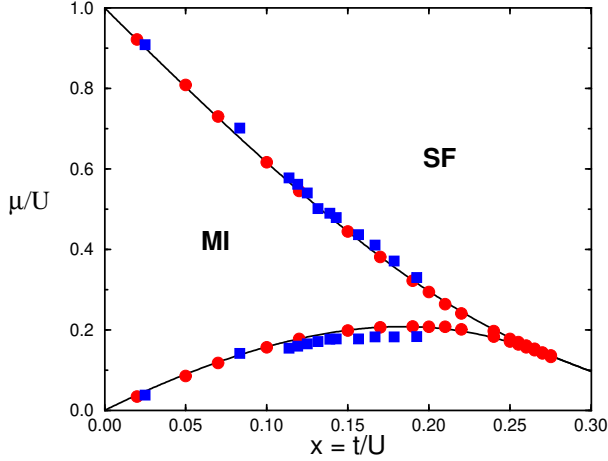


FIG. 11. Phase Diagram of the Bose-Hubbard chain: Numerical data from DMRG (light circles, ref.<sup>(12)</sup>) and QMC studies (dark squares, ref.<sup>(2)</sup>) compared to the results of a Pade analysis.

1  
X

$$H(1,1) = 1$$

1 2  
X X

$$H(1,1) = 1 + 0x + 5/2x^2$$

$$H(1,2) = 0 + 2x + 0x^2 - 3/2x^3$$

$$H(2,1) = 0 + 2x + 0x^2 - 3/2x^3$$

$$H(2,2) = 1 + 0x + 5/2x^2$$

1 2 3  
X X X

$$H(1,1) = 1 + 0x + 5/2x^2$$

$$H(1,2) = 0 + 2x + 0x^2 - 21/2x^3$$

$$H(1,3) = 0 + 0x - 2x^2$$

$$H(2,1) = 0 + 2x$$

$$H(2,2) = 1 + 0x + 5x^2$$

$$H(2,3) = 0 + 2x$$

$$H(3,1) = 0 + 0x - 2x^2$$

$$H(3,2) = 0 + 2x + 0x^2 - 21/2x^3$$

$$H(3,3) = 1 + 0x + 5/2x^2$$

1 2 3 4  
X X X X

$$H(1,1) = 1 + 0x + 5/2x^2$$

$$H(1,2) = 0 + 2x + 0x^2 - 21/2x^3$$

$$H(1,3) = 0 + 0x - 2x^2$$

$$H(1,4) = 0 + 0x - 0x^2 + 6x^3$$

$$H(2,1) = 0 + 2x$$

$$H(2,2) = 1 + 0x + 5x^2$$

$$H(2,3) = 0 + 2x + 0x^2 - 9x^3$$

$$H(2,4) = 0 + 0x - 2x^2$$

$$H(3,1) = 0 + 0x - 2x^2$$

$$H(3,2) = 0 + 2x + 0x^2 - 9x^3$$

$$H(3,3) = 1 + 0x + 5x^2$$

$$H(3,4) = 0 + 2x$$

$$H(4,1) = 0 + 0x - 0x^2 + 6x^3$$

$$H(4,2) = 0 + 0x - 2x^2$$

$$H(4,3) = 0 + 2x + 0x^2 - 21/2x^3$$

$$H(4,4) = 1 + 0x + 5/2x^2$$

The cluster hamiltonians are not hermitian in all orders of the expansions. While this looks strange at first sight it is just a consequence of the finite cluster size which lacks the translational symmetry of the full lattice. Therefore the sites of a finite cluster are no longer all equal and so the sequence of intermediate virtual states that connects two different sites  $i$  and  $j$  depends on the actual order, i.e. in perturbation theory going from site  $i$  to site  $j$  is not equivalent to going from  $j$  to  $i$ . An example is the following sequence of states that contributes in third order to  $H(1,2)$  the hamiltonian of the two bond cluster:

$$|2, 1, 1\rangle \rightarrow |2, 2, 0\rangle \rightarrow |1, 3, 0\rangle \rightarrow |1, 2, 1\rangle$$

In the contribution to  $H(2,1)$  the same intermediate states will contribute but in reverse order and this gives rise to the non hermitian cluster hamiltonian. There is no equivalent sequence to the one shown above, because the sites 1 and 2 are not equivalent. When the effective hamiltonian for the full lattice will be calculated later on all embeddings of the cluster into the lattice have to be taken into account. This restores the translational symmetry and the resulting Hamiltonian will be hermitian again.

A new complication arises when performing the sub-cluster subtraction, because matrix elements have to be subtracted and it is therefore necessary to keep track of exactly which sites of a cluster are covered by the sites in a particular subcluster. The subtraction procedure is shown in the following graph.

$$\begin{array}{c} \begin{array}{c} 1 \quad 2 \\ \bullet \text{---} \bullet \end{array} \\ \\ \begin{array}{c} \text{---} \\ \begin{array}{cc} \begin{array}{c} 1 \\ (1) \end{array} & \begin{array}{c} 2 \\ (1) \end{array} \end{array} \end{array} = \begin{array}{c} \begin{array}{c} 1 \quad 2 \\ \times \text{---} \times \end{array} \\ \\ \begin{array}{c} \text{---} \\ \begin{array}{cc} \begin{array}{c} 1 \\ (1) \end{array} & \begin{array}{c} 2 \\ (1) \end{array} \end{array} \end{array}$$



$$\begin{array}{c}
\begin{array}{ccc} 1 & 2 & 3 \\ \bullet & \bullet & \bullet \end{array} \\
= \\
\begin{array}{ccc} 1 & 2 & 3 \\ \times & \times & \times \end{array} \\
- \\
\begin{array}{ccc} 1 & 2 & 3 \\ (1) & (1) & (1) \end{array} \\
- \\
\begin{array}{ccc} 1 & 2 & 3 \\ (1) & (2) & \circ \end{array} \\
- \\
\begin{array}{ccc} 1 & 2 & 3 \\ \circ & (1) & (2) \end{array}
\end{array}$$

The subtraction procedure gives the cluster weights of the hamiltonian and as it is the case for the ground state energy the weights for a cluster with  $n$ -bonds are at least of order  $\mathcal{O}(x^n)$ .

$$\begin{array}{c} 1 \\ \bullet \end{array}$$

$$W_H(1, 1) = 1$$

$$\begin{array}{cc} 1 & 2 \\ \bullet & \bullet \end{array}$$

$$W_H(1, 1) = 0 + 0x + 5/2 x^2$$

$$W_H(1, 2) = 0 + 2x + 0x^2 - 3/2 x^3$$

$$W_H(2, 1) = 0 + 2x + 0x^2 - 3/2 x^3$$

$$W_H(2, 2) = 0 + 0x + 5/2 x^2$$

$$\begin{array}{ccc} 1 & 2 & 3 \\ \bullet & \bullet & \bullet \end{array}$$

$$W_H(1, 2) = 0 + 0x + 0x^2 - 9x^3$$

$$W_H(1, 3) = 0 + 0x - 2x^2 + 0x^3$$

$$W_H(2, 1) = 0 + 0x + 0x^2 + 3/2 x^3$$

$$W_H(2, 3) = 0 + 0x + 0x^2 + 3/2 x^3$$

$$W_H(3, 1) = 0 + 0x - 2x^2 + 0x^3$$

$$W_H(3, 2) = 0 + 0x + 0x^2 - 9x^3$$

$$\begin{array}{cccc} 1 & 2 & 3 & 4 \\ \bullet & \bullet & \bullet & \bullet \end{array}$$

$$W_H(1, 4) = 0 + 0x + 0x^2 + 6x^3$$

$$W_H(4, 1) = 0 + 0x + 0x^2 + 6x^3$$

The last steps requires to find all possible embeddings of the cluster in the chain. Due to the translational invariance of the problem, it is sufficient to search only those possibilities where that connect the origin to other sites. For the first clusters this is demonstrated in the following:

$$\begin{array}{cccccc} -3 & -2 & -1 & 0 & 1 & 2 & 3 \\ \circ & \circ & \circ & \bullet & \circ & \circ & \circ \\ & & & (1) & & & \end{array}$$

$$\begin{array}{cccccc} -3 & -2 & -1 & 0 & 1 & 2 & 3 \\ \circ & \circ & \circ & \bullet & \bullet & \circ & \circ \\ & & & (1) & (2) & & \end{array}$$

$$\begin{array}{cccccc} -3 & -2 & -1 & 0 & 1 & 2 & 3 \\ \circ & \circ & \circ & \bullet & \circ & \circ & \circ \\ & & & (1) & (2) & & \end{array}$$

$$\begin{array}{cccccc} -3 & -2 & -1 & 0 & 1 & 2 & 3 \\ \circ & \circ & \circ & \bullet & \bullet & \bullet & \circ \\ & & & (1) & (2) & (3) & \end{array}$$

$$\begin{array}{cccccc} -3 & -2 & -1 & 0 & 1 & 2 & 3 \\ \circ & \circ & \circ & \bullet & \bullet & \bullet & \circ \\ & & & (1) & (2) & (3) & \end{array}$$

$$\begin{array}{cccccc} -3 & -2 & -1 & 0 & 1 & 2 & 3 \\ \circ & \bullet & \bullet & \bullet & \circ & \circ & \circ \\ & (1) & (2) & (3) & & & \end{array}$$

Up to third order in the expansion parameter the effective hamiltonian for the single particle states in the Bose-Hubbard chain reads:

$$H_{\text{eff}}(-3) = 0 + 0x + 0x^2 + 6x^3$$

$$H_{\text{eff}}(-2) = 0 + 0x - 2x^2 + 0x^3$$

$$H_{\text{eff}}(-1) = 0 + 2x + 0x^2 - 9x^3$$

$$H_{\text{eff}}(0) = 1 + 0x + 5x^2 + 6x^3$$

$$H_{\text{eff}}(1) = 0 + 2x + 0x^2 - 9x^3$$

$$H_{\text{eff}}(2) = 0 + 0x - 2x^2 + 0x^3$$

$$H_{\text{eff}}(3) = 0 + 0x + 0x^2 + 6x^3$$

Note that the effective hamiltonian is hermitian.

## APPENDIX B: HASH FUNCTION FOR LATTICE BOSONS

Perturbation theory requires to work in the full hilbert space of the finite clusters. It is therefore necessary to have an efficient method to represent the basis and the hamiltonian. In particular there is a need for a Hash function that labels each basis state in a unique way. The hamiltonian (1) conserves the total particle number  $N$ . For a cluster with  $L$  sites and fixed  $N$  the hilbert space has a total of

$$D(N, L) = \frac{(N + L - 1)!}{N! (L - 1)!} \quad (\text{B1})$$

states. The natural basis is given by the set of occupation numbers  $\{n_i\}$  of all lattice sites  $i$ ,  $|n_1, n_2, n_3, \dots, n_L\rangle$ . We now describe how to construct the full basis. The first state is the one where all particles are sitting on site 1. Then follow those states where the first two sites are occupied. In the next step the last occupied site is  $i = 3$ . From those possibilities we first get all those with just one boson on site 3. There are then three bosons left

to be distributed on  $i = 1$  and  $i = 2$  and we repeat the procedure, first all three on site 1 and so on.

Define

$$\theta_i := \sum_{j=1}^i n_j \quad , \quad \theta_0 := 0 \quad (\text{B2})$$

Which is related to the occupation number by

$$n_i = \theta_i - \theta_{i-1} \quad (\text{B3})$$

Hash function

$$Hf(\{n_i\}) = \sum_{j=1}^L [D(\theta_i, i) - D(\theta_{i-1}, i)] \quad (\text{B4})$$

- 
- <sup>1</sup> R. T. Scalettar, G. G. Batrouni and G. T. Zimany, Phys. Rev. Lett **66**, 3144 (1991)
- <sup>2</sup> G. G. Batrouni and R. T. Scalettar, Phys. Rev. B **46**, 9051 (1992)
- <sup>3</sup> P. Niyaz, R. T. Scalettar, C. Y. Fong and G. G. Batrouni, Phys. Rev. B **50**, 362 (1994)
- <sup>4</sup> W. Krauth and N. Trivedi, Europhys. Lett **14**, 627 (1991)
- <sup>5</sup> W. Krauth, N. Trivedi and D. Ceperley, Phys. Rev. Lett **67**, 2307 (1991)
- <sup>6</sup> A. van Otterlo and K.-H. Wagenblast, Phys. Rev. Lett **72**, 3598 (1994)
- <sup>7</sup> G. G. Batrouni, R. T. Scalettar, G. T. Zimany and A. P. Kampf, Phys. Rev. Lett **72**, 3598 (1994)
- <sup>8</sup> M. P. Gelfand, R. R. P. Singh, and D. A. Huse, J. Stat. Phys. **59**, 1093 (1990)
- <sup>9</sup> M. P. Gelfand, Sol. Stat. Com. **98**, 11 (1996)
- <sup>10</sup> M. P. A. Fisher, P. B. Weichman, G. Grinstein, and D. S. Fisher, Phys. Rev. B **40**, 546 (1989).
- <sup>11</sup> T. Kühner, diploma thesis, Bonn University (1997)
- <sup>12</sup> T. Kühner, and H. Monien, preprint, cond-mat/9712307
- <sup>13</sup> J. C. Le Guillou, and J. Zinn-Justin, Phys. Rev. Lett. **39**, 95 (1977)
- <sup>14</sup> B. G. Orr, H. M. Jaeger, A. M. Goldman, and C. G. Kuper, Phys. Rev. Lett. **56**, 378 (1986); D. B. Haviland, Y. Liu, and A. M. Goldman, Phys. Rev. Lett. **62**, 2180 (1989); H. M. Jaeger, D. B. Haviland, B. G. Orr, and A. M. Goldman, Phys. Rev. B **40**, 182 (1989).
- <sup>15</sup> A. Oudenaarden and J. E. Mooij, Phys. Rev. Lett. **76**, 4947 (1996).
- <sup>16</sup> R. Baltin and K.-H. Wagenblast, Europhys. Lett. **39**, 7 (1997); L. I. Glazman and A. I. Larkin, Phys. Rev. Lett. **79**, 3736 (1997).
- <sup>17</sup> S. R. White, Phys. Rev. Lett. **69**, 2863 (1992).
- <sup>18</sup> Pai et al.<sup>22</sup> have chosen a cut-off of four particle per site for the same phase. Kashurnikov and Svistunov<sup>26</sup> found  $n = 3$  to be very close to the full model.
- <sup>19</sup> V. L. Berezinskii, Zh. Eksp. Teor. Fiz. **61**, 1144 (1971) [JETP **34**, 610 (1972)]; J. M. Kosterlitz and D. J. Thouless, Journal of Physics C **6**, 1181 (1973); J. M. Kosterlitz, Journal of Physics C **7**, 1046 (1974).
- <sup>20</sup> V. F. Elesin, V. A. Kashurnikov, and L. A. Openov, Pis'ma Zh. Eksp. Teor. Fiz. **60**, 174 (1994) [JETP Lett. **60**, 177 (1994)].
- <sup>21</sup> V. A. Kashurnikov, A. V. Krasavin, and B. V. Svistunov, Pis'ma Zh. Eksp. Theo. Fiz. **64**, 92 (1996) [JETP Lett. **64**, 99 (1996)].
- <sup>22</sup> R. V. Pai, R. Pandit, H. R. Krishnamurthy, and S. Ramasesha, Phys. Rev. Lett. **76**, 2937 (1996).
- <sup>23</sup> F. D. M. Haldane, Physics Review Letters **47**, 1840 (1981); F. D. M. Haldane, J.Phys.C **14**, 2585 (1981).
- <sup>24</sup> T. Giamarchi and A. J. Millis, Phys. Rev. B **46**, 9325 (1992).
- <sup>25</sup> W. Krauth, Phys.Rev.B **44**, 9772 (1991).
- <sup>26</sup> V. A. Kashurnikov and B. V. Svistunov, Phys. Rev. B **53**, 11776 (1996).
- <sup>27</sup> G. G. Batrouni and R. T. Scalettar, Phys. Rev. B **46**, 9051 (1992).
- <sup>28</sup> J. K. Freericks and H. Monien, Phys. Rev. B **53**, 2691 (1996).
- <sup>29</sup> M. W. Meisel, Physica B **178**, 121 (1992); G. G. Batrouni, R. T. Scalettar, G. T. Zimanyi, and A. P. Kampf, Phys. Rev. Lett. **74**, 2527 (1995).

TABLE I. Series for the single particle gap  $\Delta$  and the equal time structure factor  $S_{\mathbf{q}=0}$  of the Bose-Hubbard model on the square lattice.

gap series	
n	$a_n$
0	1
1	-12
2	-22
3	-264
4	-15659 / 10
5	-656984 / 25
6	-513092341 / 2250
7	-13396365654 / 3375
8	-2194497431888101 / 56700000
9	-523244582353596437 / 744187500
10	-4749112579154967367231 / 625117500000
11	-6676218845916748474723399 / 49228003125000
12	-5669114326328304841982042447 / 3508972062750000
13	-3473317126780784521271398100 / 126449317253259
structure factor series	
n	$a_n$
0	3
1	32
2	432
3	6656
4	99632
5	14154496 / 9
6	663550400 / 27
7	31905307840 / 81
8	7618958766796 / 1215
9	12934227681606432 / 127575
10	14570617373829713351 / 8930250
11	19905912307529372064253 / 750141000
12	17231660529006598072716626038 / 40068302174901
13	47514032474492554578981737799.4028 / 6764778289269

TABLE II. Series for the single particle gap  $\Delta$  and the equal time structure factor  $S_{\mathbf{q}=0}$  of the Bose-Hubbard model on the triangular lattice.

gap series	
n	$a_n$
0	1
1	-18
2	-81
3	-819
4	-54891 / 4
5	-11459377 / 50
6	-6764830501 / 1500
7	-3957593443549 / 45000
8	-23724030434424597 / 12600000
9	-79054659543137812691 / 1984500000
10	-49507676563116513700717 / 55566000000
11	-19752788544107.0312336222045518956
12	-454652221307484.008486685913608139
13	-10398395856680122.5582305335816799
structure factor series	
n	$a_n$
0	3
1	48
2	1080
3	25344
4	613016
5	15108128
6	3391856144 / 9
7	28444402112 / 3
8	97228564590772 / 405
9	86595555599744452 / 14175
10	2787620342817465447617 / 17860500
11	82527451969123616224435919 / 20628877500
12	102821325219551430.224270929006395
13	2648736908451106507.61278132531748

TABLE III. Series for the single particle gap  $\Delta$  and the equal time structure factor  $S_{\mathbf{q}=0}$  of the Bose-Hubbard chain.

gap series	
n	$a_n$
0	1
1	-6
2	5
3	6
4	287 / 20
5	17463 / 150
6	-1806729 / 3000
7	73674531 / 22500
8	-297690613629 / 16200000
9	14666046468323 / 121500000
10	-6295148943458549 / 7290000000
11	114441271150219589 / 18225000000
12	-422231271662550684871 / 9185400000000
13	1473292023890353319230511 / 4340101500000000

structure factor series	
n	$a_n$
0	3
1	16
2	72
3	320
4	4120 / 3
5	48544 / 9
6	596992 / 27
7	2396512 / 27
8	27653840 / 81
9	1329678
10	22598877209 / 4375
11	1275342277201 / 65610
12	4055776421430107 / 55112400
13	203597243119484303 / 723350250

TABLE IV. D-log Pade approximants for the critical point  $t_c$  and the critical exponents  $\nu$  and  $\gamma_s$  of the Bose-Hubbard model on the square lattice.

[L/M]	gap		structure factor	
	$t_c$	$\nu$	$t_c$	$\gamma_s$
[4/4]	0.05980859	0.69137519	0.05976303	0.65480784
[4/5]	0.05978709	0.68924487	0.05976978	0.65534864
[5/4]	0.05980549	0.69112808	0.05971761	0.65393342
[4/6]	0.05980887	0.69140624	0.05976747	0.65515773
[5/5]	0.05980805	0.69133305	0.05976666	0.65508534
[6/4]	0.05980880	0.69140183	0.05976814	0.65522423
[4/7]	0.05980331	0.69097429	0.05975849	0.65433135
[5/6]	0.05984310	0.69384313	0.05978395	0.65596948
[6/5]	0.05980488	0.69108539	0.05976313	0.65477892
[7/4]	0.05980859	0.69138480	0.05976778	0.65519366
[4/8]	0.05978512	0.68975552	0.05974697	0.65294432
[5/7]	0.05987138	0.69556354	0.05973294	0.65050768
[6/6]	0.05987084	0.69552706	0.05972443	0.64864666
[7/5]	0.05978277	0.68960137	0.05975399	0.65386465
[8/4]	0.06016134	0.72645361	0.05974142	0.65212846

TABLE V. D-log Pade approximants for the critical point  $t_c$  and the critical exponents  $\nu$  and  $\gamma_s$  of the Bose-Hubbard model on the triangular lattice.

[L/M]	gap		structure factor	
	$t_c$	$\nu$	$t_c$	$\gamma_s$
[4/4]	0.03781415	0.68753874	0.03768377	0.60598248
[4/5]	0.03782464	0.68812741	0.03778221	0.65202471
[5/4]	0.03777127	0.67855607	0.03778121	0.65179657
[4/6]	0.03780279	0.68619855	0.03777688	0.65066891
[5/5]	0.03780194	0.68605142	0.03777941	0.65137574
[6/4]	0.03780562	0.68666551	0.03777913	0.65130264
[4/7]	0.03779156	0.68397787	0.03777917	0.65130976
[5/6]	0.03776841	0.67611321	0.03777930	0.65134670
[6/5]	0.03779251	0.68419813	0.03777930	0.65134598
[7/4]	0.03778693	0.68276629	0.03777931	0.65134883
[4/8]	0.03778359	0.68180328	0.03777864	0.65116474
[5/7]	0.03778045	0.68074745	0.03777854	0.65113450
[6/6]	0.03778034	0.68070944	0.03777943	0.65137873
[7/5]	0.03778358	0.68180026	0.03777915	0.65130775
[8/4]	0.03778162	0.68114199	0.03777683	0.65058408